





## BRIEF DEFINITIVE REPORT

# Posttranscriptional regulation of ILC2 homeostatic function via tristetraprolin

Yuki Hikichi<sup>1,2</sup> , Yasutaka Motomura<sup>1,3,4</sup> , Osamu Takeuchi<sup>5</sup> , and Kazuyo Moro<sup>1,2,3,4</sup> 

Group 2 innate lymphoid cells (ILC2s) are unique in their ability to produce low levels of type 2 cytokines at steady state, and their production capacity is dramatically increased upon stimulation with IL-33. However, it is unknown how constitutive cytokine production is regulated in the steady state. Here, we found that tristetraprolin (TTP/Zfp36), an RNA-binding protein that induces mRNA degradation, was highly expressed in naive ILC2s and was downregulated following IL-33 stimulation. In ILC2s from *Zfp36*<sup>-/-</sup> mice, constitutive IL-5 production was elevated owing to the stabilization of its mRNA and resulted in an increased number of eosinophils in the intestine. Luciferase assay demonstrated that TTP directly regulates *Il5* mRNA stability, and overexpression of TTP markedly suppressed IL-5 production by ILC2s, even under IL-33 stimulation. Collectively, TTP-mediated posttranscriptional regulation acts as a deterrent of excessive cytokine production in steady-state ILC2s to maintain body homeostasis, and downregulation of TTP may contribute to massive cytokine production under IL-33 stimulation.

## Introduction

Group 2 innate lymphoid cells (ILC2s) produce type 2 cytokines in an antigen-independent manner (Moro et al., 2010; Neill et al., 2010; Price et al., 2010; Halim et al., 2012) and contribute to the initiation and exacerbation of type 2 inflammatory processes, such as allergic diseases and helminth infections, by producing massive amounts of IL-5 and IL-13, which induce eosinophilia and goblet cell hyperplasia, respectively. We have previously reported that *Il5* and *Il13* transcription in activated ILC2s is mediated by the phosphorylation of p38 MAPK and GATA3 downstream of IL-25 and IL-33 and by phosphorylated GATA3 bound to the promoter regions of *Il5* and *Il13* loci (Furusawa et al., 2013). ILC2s also produce small amounts of IL-5 and IL-13 in steady state. Such constitutive IL-5 and IL-13 production contributes to the self-renewal of B1 cells in the peritoneal cavity and maintenance of eosinophils in the small intestine (SI) and supports remodeling of epithelial cells in the intestine, respectively (Moro et al., 2010; Zhu et al., 2019; Nussbaum et al., 2013). Constitutive IL-5 production from ILC2s stops upon fasting and is regulated by vasoactive intestinal peptide, which is one of the intestinal peptides secreted after food intake (Nussbaum et al., 2013). A study using IL-5-deficient mice has shown that the homeostasis of eosinophils in the SI is

dependent on IL-5 (Mishra et al., 1999), and eosinophils in steady state contribute to the regulation of microbiota composition by supporting IgA production in the SI (Chu et al., 2014; Jung et al., 2015). The number of cytokines involved in homeostasis is strictly regulated since excessive cytokine production can induce homeostatic imbalance. However, the molecular mechanisms regulating the constitutive type 2 cytokine production in ILC2s are poorly understood.

Gene expression is regulated at both the transcriptional and the posttranscriptional level. Recent studies have shown the importance of posttranscriptional regulation, particularly mRNA degradation and translation, in controlling immune responses and maintaining immune homeostasis (Anderson, 2008; Fu and Blakeshear, 2017). Many cytokine-encoding mRNAs are known to be unstable owing to the presence of cis elements, such as adenine and uridine-rich elements (AREs), and stem-loop structures in their 3' untranslated regions (UTRs). These cis elements interact with RNA-binding proteins (RBPs) that regulate mRNA stability. Tristetraprolin (TTP) is one of the best-characterized RBPs and plays a role in various cells, such as macrophages, dendritic cells, T cells, and fibroblasts (Brooks and Blakeshear, 2013). Here, we found that naive ILC2s,

<sup>1</sup>Laboratory for Innate Immune Systems, RIKEN Center for Integrative Medical Sciences, Yokohama, Kanagawa, Japan; <sup>2</sup>Division of Immunobiology, Department of Medical Life Science, Graduate School of Medical Life Science, Yokohama City University, Yokohama, Kanagawa, Japan; <sup>3</sup>Laboratory for Innate Immune Systems, Department of Microbiology and Immunology, Graduate School of Medicine, Osaka University, Suita, Osaka, Japan; <sup>4</sup>Laboratory for Innate Immune Systems, Osaka University Immunology Frontier Research Center, Suita, Osaka, Japan; <sup>5</sup>Department of Medical Chemistry, Graduate School of Medicine, Kyoto University, Sakyo-ku, Kyoto, Japan.

Correspondence to Kazuyo Moro: [moro@ilc.med.osaka-u.ac.jp](mailto:moro@ilc.med.osaka-u.ac.jp); Yasutaka Motomura: [motomura@ilc.med.osaka-u.ac.jp](mailto:motomura@ilc.med.osaka-u.ac.jp).

© 2021 Hikichi et al. This article is distributed under the terms of an Attribution–Noncommercial–Share Alike–No Mirror Sites license for the first six months after the publication date (see <http://www.rupress.org/terms/>). After six months it is available under a Creative Commons License (Attribution–Noncommercial–Share Alike 4.0 International license, as described at <https://creativecommons.org/licenses/by-nc-sa/4.0/>).

but not activated ILC2s, highly express TTP to degrade extra *Il5* mRNAs in the steady state to maintain homeostasis.

## Results and discussion

### IL-33 stabilizes *Il5* and *Il13* mRNA via p38 MAPK to induce cytokine production in ILC2s

While most immune cells produce cytokines during inflammation, ILC2s are unique in that they can produce cytokines even in the steady state. Conversely, IL-33-induced inflammation results in rapid and massive cytokine production by ILC2s, suggesting that ILC2s have a great cytokine production ability in both steady state and activated state (Moro et al., 2010, 2016). We confirmed that although there are some quantitative differences between tissues, ILC2s in all tissues produce large amounts of IL-5 and IL-13 upon stimulation with IL-33, and they produce small amounts of these cytokines constitutively in the presence of IL-7, a cytokine that maintains the survival of ILC2s without inducing activation (Fig. 1 A). Phosphorylation peaks 30 min after IL-33 stimulation and subsequently decreases, whereas type 2 cytokine production in ILC2s in response to IL-33 continues even after phosphorylation levels diminish (Furusawa et al., 2013). These results strongly suggest that regulatory mechanisms, other than those affecting transcription, sustain type 2 cytokine production, resulting in high levels in ILC2s. To assess this possibility, we first compared the kinetics of IL-5 and IL-13 production and the expression of pre-mRNA, an RNA product before processing (to assess transcriptional activity), as well as total mRNA levels of *Il5* and *Il13* in ILC2s under IL-33 stimulation. Consistent with large IL-5 and IL-13 production in ILC2s (Fig. 1 B), the *Il5* and *Il13* total mRNA levels remained high at 72 h compared with baseline levels (Fig. 1 C). However, the levels of *Il5* primary transcripts peaked 3 h after IL-33 stimulation and decreased to baseline levels by 72 h, whereas the *Il13* primary transcript level continued to increase until 72 h after IL-33 stimulation (Fig. 1 D).

Among the several posttranscriptional regulatory steps in cytokine production, mRNA stability regulated by p38 MAPK is well reported in various cell types, including immune cells (Dean et al., 2004; Venigalla and Turner, 2012). We determined whether p38 MAPK is involved in stabilizing *Il5* and *Il13* mRNAs in ILC2s. Consistent with a previous report (Furusawa et al., 2013), SB203580, a p38 inhibitor, considerably reduced the production of IL-5 and IL-13 and *Il5* and *Il13* mRNA levels upon IL-33 stimulation in ILC2s without affecting cell viability (Fig. 1, E–G). To elucidate whether mRNA degradation is involved in suppressing type 2 cytokine gene expression by SB203580 in ILC2s, we measured the stability of *Il5* and *Il13* mRNAs after blocking the p38 MAPK pathway in IL-33-stimulated ILC2s. Interestingly, increased *Il5* and *Il13* mRNA degradation was observed in the presence of SB203580 compared with the control (Fig. 1 H), suggesting that IL-33 signaling stabilizes *Il5* and *Il13* mRNAs via p38 MAPK to enhance type 2 cytokine production in ILC2s.

### ILC2s highly express the RBP TTP under steady-state conditions

To identify the genes that control type 2 cytokine gene expression at the posttranscriptional level, we compared the

transcriptome of naive and IL-33-stimulated ILC2s by RNA sequencing analysis. One of the most remarkable differentially expressed genes between naive and activated ILC2s was zinc finger protein 36 (*Zfp36*), which encodes the RBP TTP (Fig. 2 A), a posttranscriptional regulator that mediates mRNA degradation (Brooks and Blakeshear, 2013). While the expression levels of genes associated with proliferation (*Mki67*) and effector molecules (*Il5*, *Il9*, *Il13*, and *Pdcd1*) were upregulated in ILC2s activated via IL-33, *Zfp36* was highly expressed in naive ILC2s and was downregulated following ILC2 activation (Fig. 2 B). In naive ILC2s, *Zfp36* was the most highly expressed among the investigated CCCH zinc finger protein genes that often function as RBPs and regulate RNA metabolism (Fig. 2 C; Liang et al., 2008; Fu and Blakeshear, 2017). In addition, *Zfp36* expression in ILC2s was higher than that in macrophages in which TTP functions are well known (Fig. 2 D; Carballo et al., 1998; Sauer et al., 2006; Stoecklin et al., 2008; Qian et al., 2011). Since ILC2s have heterogeneity among different tissues (Moro et al., 2015; Ricardo-Gonzalez et al., 2018), we compared the expression of *Zfp36* in ILC2s from different peripheral tissues (Fig. 2 E). In each tissue type, ILC2s expressed *Zfp36* at high levels under steady-state conditions, suggesting that TTP exerts a broad effect in all peripheral tissue resident ILC2s. Consistent with RNA sequencing data, the expression of *Zfp36* in ILC2s was the highest among all ILC subsets (Fig. 2 F). Moreover, quantitative PCR (qPCR) analysis confirmed that *Zfp36* expression was reduced in activated ILC2s under IL-33 stimulation both in vitro (Fig. 2 G) and in vivo (Fig. 2 H), and in vivo experiments showed an inverse correlation between *Zfp36* and *Il5* and *Il13* expressions. These data suggest that TTP acts as a posttranscriptional regulator that negatively controls type 2 cytokine gene expression in ILC2s in the steady state, and downregulation of TTP by IL-33 stimulation may contribute to enhanced production of type 2 cytokines in ILC2s.

### TTP negatively regulates IL-5 and IL-13 production via mRNA degradation

TTP targets several mRNAs that encode cytokines and chemokines (Brooks and Blakeshear, 2013); however, it is unclear whether *Il5* and *Il13* mRNAs are the targets of TTP. To further elucidate the regulatory mechanism of type 2 cytokine gene expression by TTP in ILC2s, after downregulating TTP in ILC2s via IL-2 and IL-33 stimulation, we overexpressed TTP using a retroviral vector. The overexpression level was within the physiological range (Fig. S1 A). TTP overexpression markedly suppressed IL-5 and IL-13 production in ILC2s stimulated with IL-2 and IL-33 (Fig. 3 A). Because ILC2s produce several cytokines, including IL-6 and GM-CSF, which have been reported as targets of TTP in macrophages and stromal cells in the bone marrow (BM; Sauer et al., 2006; Carballo et al., 2000), we performed multiplex assays in TTP-overexpressing ILC2s to identify cytokines regulated by TTP. In addition to IL-5 and IL-13, IL-6 and GM-CSF production under IL-2 plus IL-33 stimulation were reduced by TTP overexpression in ILC2s (Fig. 3 B). Consistent with the multiplex assay results, *Il5*, *Il6*, and *Il13* levels were decreased in TTP-overexpressing ILC2s (Fig. 3 C). However, the expression of *Csf2* was not suppressed by TTP overexpression, presumably because TTP suppresses *Csf2* translation

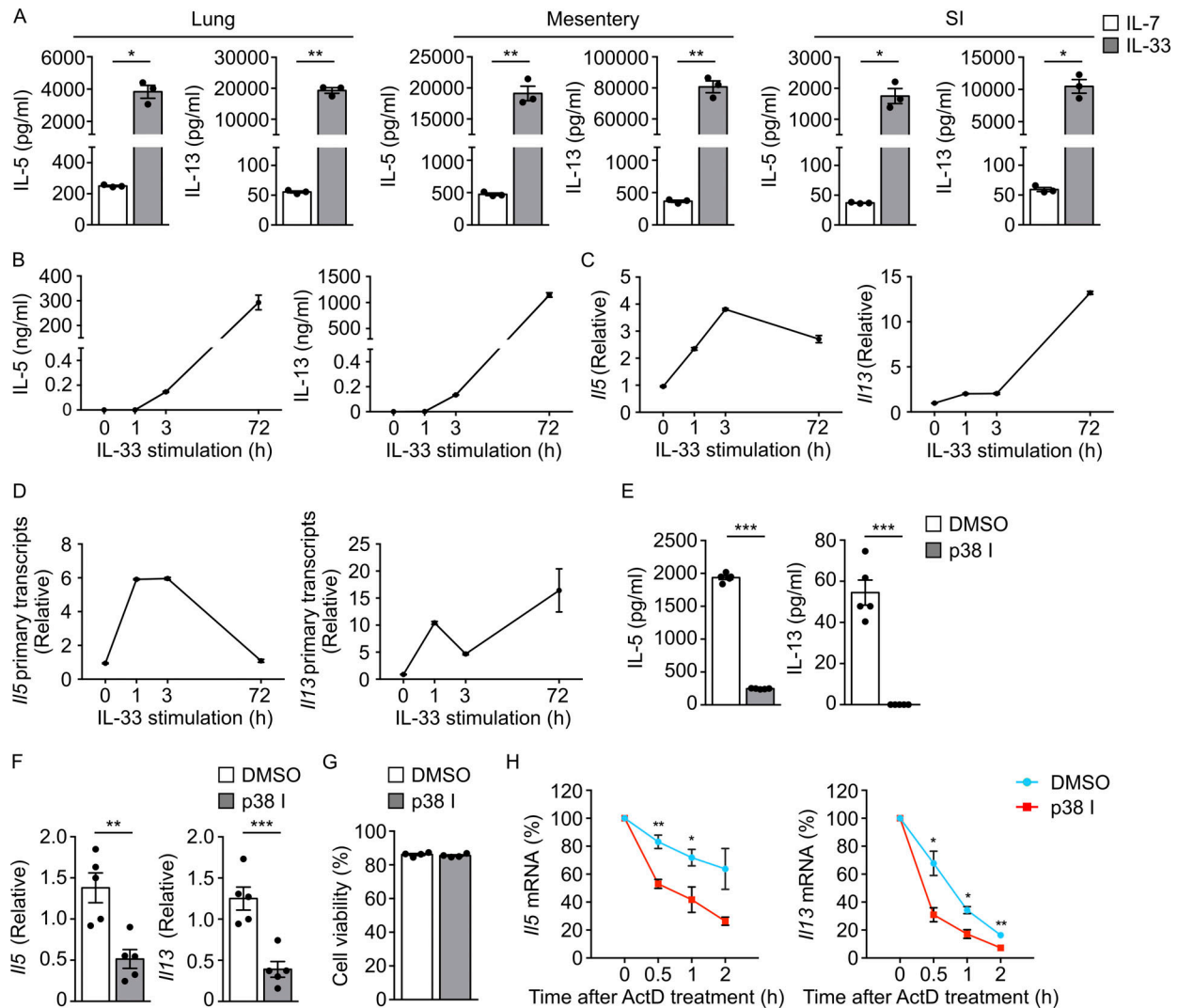


**Figure 1. IL-33 stabilizes *IL5* and *IL13* mRNAs via p38 MAPK to induce cytokine production in ILC2s.** (A) Concentration of IL-5 and IL-13 in the supernatants of isolated ILC2s ( $1.5 \times 10^4$  cells) from the lungs, mesentery, or SI cultured with IL-7 or IL-33 for 48 h, as determined by ELISA. (B–D) Isolated ILC2s ( $3 \times 10^4$  cells) from the mesentery cultured with IL-33 for 0–72 h. (B) Concentrations of IL-5 and IL-13 in the culture supernatants at the indicated time points, as determined by ELISA. (C) Expression levels of *IL5* and *IL13* in ILC2s at the indicated time points, as measured by qPCR. (D) Expression levels of *IL5* and *IL13* primary transcripts in ILC2s at the indicated time points, as measured by qPCR. (E–G) Isolated ILC2s ( $3 \times 10^4$  cells) from the mesentery pretreated with DMSO or p38 inhibitor (p38 I; SB203580) for 1 h and stimulated with IL-33 for 12 h. (E) Concentrations of IL-5 and IL-13 in the culture supernatants, as determined by ELISA. (F) Expression levels of *IL5* and *IL13* in ILC2s measured by qPCR. (G) Cell viability at the end of stimulation. (H) Expression levels of *IL5* and *IL13* mRNA in isolated ILC2s from the mesentery, which was prestimulated with IL-33 for 2 h and then treated with actinomycin D (ActD) and p38 I for 0.5, 1, and 2 h under IL-33-stimulated conditions, as measured by qPCR. Data are representative of two independent experiments (mean  $\pm$  SEM of  $n = 3$  or 5). \*,  $P < 0.05$ ; \*\*,  $P < 0.01$ ; \*\*\*,  $P < 0.001$  by Student's *t* test.

through a general translation repressor RCK (Grosset et al., 2004; Qi et al., 2012). We also evaluated the mRNA stability of *IL5*, *IL6*, and *IL13* and found that mRNA degradation was enhanced by TTP overexpression (Fig. 3 D). Notably, overexpression of TTP markedly enhanced the degradation of both *IL5* and *IL13* mRNAs, consistent with their reduced mRNA expression and protein production in TTP-overexpressing ILC2s (Fig. 3, B and C). Collectively, these results suggest that TTP regulates *IL5*, *IL6*, and *IL13* expression in ILC2s through mRNA degradation.

TTP directly regulates the stability of *IL6* mRNA by targeting its AREs in the 3' UTR (Zhao et al., 2011); however, it remains unknown whether TTP also directly regulates *IL5* and *IL13*

mRNAs, which also have AREs in the 3' UTR of their mRNAs (Fig. S1 B). To assess the binding capacity of TTP to 3' UTR of *IL5* and *IL13* mRNAs, we performed luciferase reporter assays with *IL5* and *IL13* 3' UTRs. We cloned the *IL5* and *IL13* 3' UTRs downstream of the luciferase gene (Fig. 3 E) and cotransfected these constructs into MEFs with a TTP-overexpressing vector. As expected, TTP decreased luciferase activity in cells transfected with the reporter plasmid containing the *IL5* 3' UTR; however, this effect was not observed with that of the *IL13* 3' UTR (Fig. 3 F). Therefore, to identify the target AREs of TTP in *IL5* 3' UTR, we generated three constructs by mutating different AREs in the *IL5* 3' UTR (Fig. 3 G) and performed a reporter assay. Luciferase

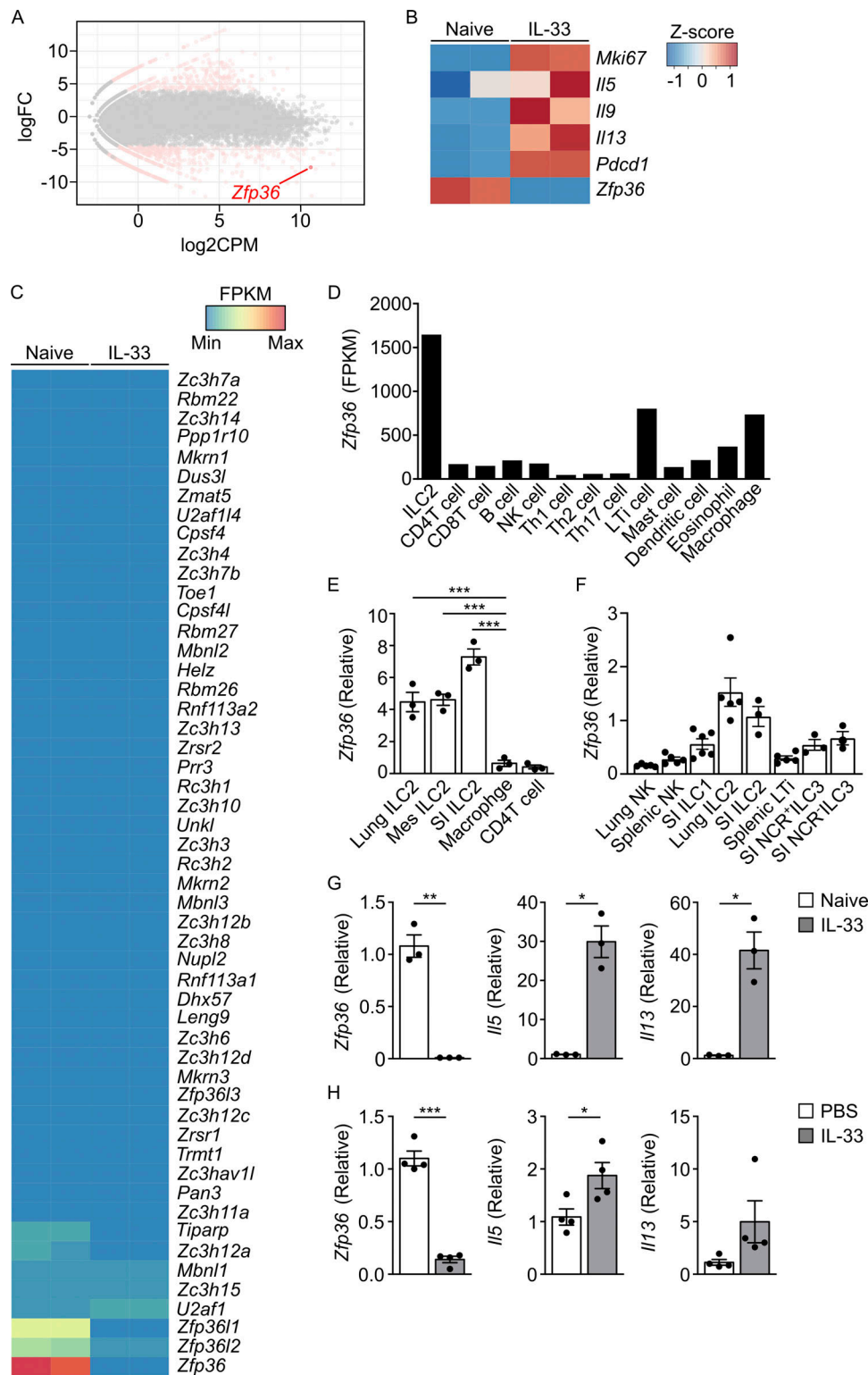


**Figure 2. ILC2s highly express the RBP TTP under steady-state conditions. (A–C)** RNA sequencing analysis of freshly isolated ILC2s from the mesentery and ILC2s isolated from the mesentery and cultured with IL-33 for 48 h. **(A)** MA plot of genes expressed in naive ILC2s versus IL-33–stimulated ILC2s. Pink dots indicate genes that were significantly differentially expressed (false discovery rate <0.01 and |Z-score| >2). CPM, counts per million mapped reads. **(B)** Heatmap of the gene expression Z-score of effector molecules in ILC2s. **(C)** Heatmap of the gene expression of CCCH zinc finger proteins in ILC2s. **(D)** Expression level of *Zfp36* in the indicated immune cells without stimulation, as detected by RNA sequencing. **(E)** Expression level of *Zfp36* in the indicated immune cells without stimulation, as measured by qPCR. **(F)** Expression level of *Zfp36* in the indicated freshly isolated ILCs, as measured by qPCR. **(G)** Expression levels of *Zfp36*, *Il5*, and *Il13* in freshly isolated ILC2s from the mesentery and ILC2s isolated from the mesentery and cultured with IL-33 for 48 h, as measured by qPCR. **(H)** Expression levels of *Zfp36*, *Il5*, and *Il13* in ILC2s isolated from the lungs of mice at 24 and 72 h after i.n. administration of PBS or IL-33, as measured by qPCR. Two independent samples were prepared for each cell population, except for dendritic cells, eosinophils, and macrophages (A–D). Data are representative of

activity in cells transfected with the *Il5* 3' UTR  $\Delta$ ARE1-3 and  $\Delta$ ARE4 constructs was significantly reduced by TTP to a similar level as that in cells cotransfected with the full-length *Il5* 3' UTR construct and the TTP-overexpressing vector (Fig. 3 H). However, cells transfected with the *Il5* 3' UTR  $\Delta$ ARE5-7 construct displayed no reduction in the luciferase activity by TTP, suggesting that ARE5-7, but not ARE1-4, contributed to the degradation of *Il5* mRNA by TTP. These data indicate that TTP directly regulates *Il5* expression and indirectly regulates *Il13* expression via mRNA degradation in ILC2s.

### TTP defect upregulates constitutive IL-5 and IL-13 production by ILC2s in vivo

Based on the above results, TTP appears to function as a negative regulator of IL-5 and IL-13 production by ILC2s. To assess the role of TTP in ILC2s in vivo, we generated *Zfp36*<sup>-/-</sup> mice in which a frameshift deletion mutation was introduced in the *Zfp36* locus using the CRISPR/Cas9 system (Fig. S2, A and B). The deletion of *Zfp36* in genomic DNA was confirmed at the mRNA and protein levels (Fig. S2, C-E). Consistent with previous reports (Taylor et al., 1996; Kaplan et al., 2011), *Zfp36*<sup>-/-</sup> mice exhibited poor growth and increased Gr-1<sup>+</sup>CD11b<sup>+</sup> cells and granulocyte-monocyte progenitors (GMPs) but differed in that T cells in the BM were reduced (Fig. S2, F and G). Meanwhile, the number of ILC2s was comparable with that in the lungs of *Zfp36*<sup>+/+</sup> mice and slightly increased compared with that in the SI of *Zfp36*<sup>-/-</sup> mice, indicating that TTP does not exert critical effects on the development of ILC2s (Fig. 4 A). As TTP expression was downregulated in ILC2s following their activation (Fig. 2, G and H), we focused on the role of TTP on IL-5 and IL-13 production in the steady state. To maintain the survival of ILC2s without activation, ILC2s from the lungs and SI of *Zfp36*<sup>-/-</sup> mice were cultured with IL-7. Contrary to the results of TTP overexpression, excessive production of IL-5 and IL-13 was observed in *Zfp36*<sup>-/-</sup> ILC2s collected from the lungs and SI without activation stimuli (Fig. 4 B), indicating that TTP restricts constitutive IL-5 and IL-13 production in ILC2s.

Because ILC2-derived IL-5 was reported to support the maintenance of eosinophils in the SI at steady state (Nussbaum et al., 2013), we analyzed the number of eosinophils in the lungs and SI of *Zfp36*<sup>-/-</sup> mice. In agreement with the increase in number of ILC2s in the SI, the accumulation of eosinophils was prominently enhanced in the SI of *Zfp36*<sup>-/-</sup> mice (Fig. 4 C). However, the number of eosinophils in the lungs of *Zfp36*<sup>-/-</sup> mice was comparable with that of *Zfp36*<sup>+/+</sup> mice, consistent with a previous study reporting that the accumulation of lung eosinophils is IL-5 dependent only under inflammatory conditions and not in the steady state (Mesnil et al., 2016). Flow cytometry demonstrated that excessive IL-5 production in *Zfp36*<sup>-/-</sup> mice was restricted to lineage (Lin)-negative cells corresponding to ILC2s (Fig. 4 D), suggesting that the number of homeostatic eosinophils in the SI is regulated by IL-5 from ILC2s via TTP. It has been reported that homeostatic eosinophils in the SI protect

the mucosal barrier by supporting IgA production from plasma cells (Chu et al., 2014; Jung et al., 2015), and indeed, we observed enhanced IgA production in the SI of *Zfp36*<sup>-/-</sup> mice (Fig. S2 H). These results suggest that TTP contributes to intestinal homeostasis by regulating the number of eosinophils through an appropriate amount of IL-5 from ILC2s.

Lung and intestinal epithelial cells are known sources of IL-33 and express TTP (Zhao et al., 2016; Eshelman et al., 2019), and TTP reportedly regulates *Il13* expression in gastric cancer (Deng et al., 2016). It is thus possible that the overproduction of IL-5 and IL-13 in ILC2s is due to the enhanced production of IL-33 from epithelial cells in *Zfp36*<sup>-/-</sup> mice. However, qPCR analysis revealed that the expression levels of *Il13* in the lungs and SI of *Zfp36*<sup>-/-</sup> mice are comparable with those of *Zfp36*<sup>+/+</sup> mice (Fig. S2 I). Additionally, there was no difference in the expression of activation markers of ILC2s in the lungs or SI of *Zfp36*<sup>+/+</sup> and *Zfp36*<sup>-/-</sup> mice, suggesting that the overproduction of IL-5 and IL-13 by ILC2s in *Zfp36*<sup>-/-</sup> mice is due to intracellular regulation rather than external activation (Fig. 4 E). To verify whether elevated IL-5 and IL-13 production in ILC2s occurred in a cell-intrinsic manner in *Zfp36*<sup>-/-</sup> mice, BM cells from WT (CD45.1) and *Zfp36*<sup>-/-</sup> (CD45.2) mice were cotransferred into *Il2rg*<sup>-/-</sup>*Rag2*<sup>-/-</sup> mice lacking all lymphocytes. The production of both IL-5 and IL-13 was increased in ILC2s derived from *Zfp36*<sup>-/-</sup> BM cells in both the lungs and the SI (Fig. 4, F and G), demonstrating that TTP regulates constitutive IL-5 and IL-13 production in ILC2s in a cell-intrinsic manner.

Finally, we evaluated the mRNA stability of *Il5* and *Il13* in ILC2s of steady-state *Zfp36*<sup>-/-</sup> mice. While *Il5* mRNA was significantly stabilized in *Zfp36*<sup>-/-</sup> ILC2s, *Il13* was only slightly stabilized (Fig. 4 H), suggesting that constitutive IL-5 production in ILC2s is negatively regulated by TTP via *Il5* mRNA degradation, while that of IL-13 is regulated by TTP not only via *Il13* mRNA degradation but also via other mechanisms. Collectively, these results indicate that TTP directly suppresses the constitutive IL-5 production by ILC2s while indirectly regulating IL-13 production. The negative regulation of ILC2s by TTP through posttranscriptional regulation is important to prevent excessive cytokine production under steady-state conditions.

Here, we identify IL-5 as a new target for TTP in ILC2s, in addition to IL-6 and GM-CSF, which have been reported in macrophages and stromal cells in the BM (Sauer et al., 2006; Carballo et al., 2000). Unlike IL-5 and IL-6, GM-CSF expression is regulated via translational repression by TTP in cooperation with a general translational repressor RCK (Grosset et al., 2004; Qi et al., 2012). These findings suggest that TTP suppresses not only inflammatory cytokines but also type 2 cytokines in ILC2s. Reporter assays indicated that although both *Il5* and *Il13* 3' UTRs contain AREs, TTP directly regulates *Il5* expression and indirectly regulates *Il13* expression in ILC2s. In addition, a reporter assay using *Il5* 3' UTR with mutated AREs demonstrated that the most important factors for enabling the interaction of TTP with the *Il5* 3' UTR is ARE5-7 with UAUUUU sequence. This finding is consistent with the report that the most preferred TTP

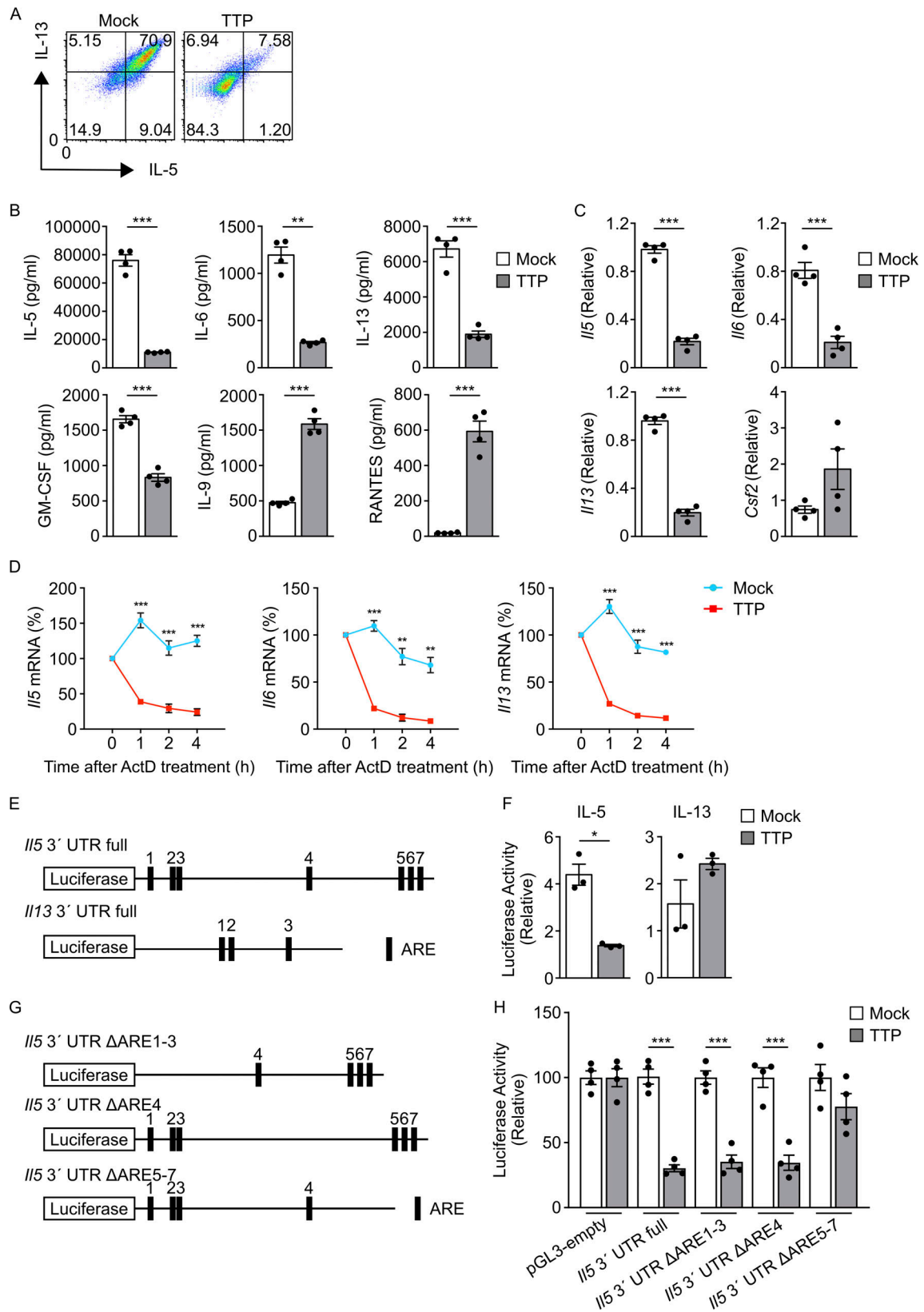


Figure 3. **TTP negatively regulates IL-5 and IL-13 production via mRNA degradation.** (A–D) IL-2-expanded ILC2s were prestimulated with IL-2 and IL-33 on day 0 and infected twice with viral particles of pMX-IRES-GFP retroviral vector encoding *Zfp36* or control vector (mock) at day 1 and day 2. GFP<sup>+</sup> cells were sorted as infected cells at day 3 for analysis in B–D. (A) Intracellular staining of IL-5 and IL-13 in the infected ILC2s at day 4 after IL-2 and IL-33 stimulation. (B) Concentrations of cytokines in the supernatants of the infected ILC2s cultured with IL-2 and IL-33 for 72 h, as determined by multiplex assay system. (C) Expression levels of *Il5*, *Il6*, *Il13*, and *Csf2* in the infected ILC2s, as measured by qPCR. (D) Expression levels of *Il5*, *Il6*, and *Il13* mRNA in the infected ILC2s

treated with actinomycin D (ActD) for 1, 2, and 4 h, as measured by qPCR. **(E)** Schematic of luciferase reporter constructs. The full-length mouse *Il5* and *Il13* 3' UTRs are downstream of the luciferase gene driven by the constitutively active SV40 promoter. **(F)** Luciferase activity in MEFs cotransfected for 48 h with indicated luciferase reporter plasmid together with control vector (mock) or retroviral vector encoding *Zfp36*. **(G)** Schematic of luciferase reporter constructs. The *Il5* 3' UTR containing  $\Delta$ AREs are downstream of the luciferase gene driven by the constitutively active SV40 promoter. **(H)** Luciferase activity in HEK293T cells cotransfected for 24 h with indicated luciferase reporter plasmid together with control vector (mock) or retroviral vector encoding *Zfp36*. Data are representative of two independent experiments (mean  $\pm$  SEM of  $n = 3$  or  $4$ ). \*,  $P < 0.05$ ; \*\*,  $P < 0.01$ ; \*\*\*,  $P < 0.001$  by two-way ANOVA with Sidak test (G) or Student's *t* test (B–F). RANTES, regulated upon activation, normal T cell expressed and presumably secreted.

binding sequence in murine primary macrophages is the UAUUUU heptamer (Sedlyarov et al., 2016). Conversely, although overexpression of TTP suppressed large amounts of IL-13 production from activated ILC2s under IL-33 stimulation, and *Zfp36*<sup>-/-</sup> mouse-derived ILC2s showed elevated IL-13 production in the steady state, reporter assays revealed that *Il13* mRNA is not a direct target of TTP.

Group 3 innate lymphoid cells (ILC3s) also express TTP (Fig. 2 F), with constitutive production of IL-22 in ILC3s reportedly controlled by circadian rhythms (Seillet et al., 2020); meanwhile, IL-22 is a target of TTP in T cells (Hårdle et al., 2015), collectively indicating that TTP may also have a similar function in ILC3s as that in ILC2s. The mechanism of homeostatic cytokine production in ILCs is not completely understood, but unlike T cells, whose cytokine production is strictly regulated in an antigen-dependent manner, ILCs readily produce cytokines, depending on various factors. Therefore, a post-transcriptional regulatory mechanism in which TTP suppresses cytokine production in the steady state and permits the production of large amounts of cytokines when necessary may be important in preventing the development of ILC-related diseases.

## Materials and methods

### Mice

All mice were maintained under specific pathogen-free conditions at the RIKEN Center for Integrative Medical Sciences (IMS) and Osaka University. C57BL/6N mice were purchased from Charles River Laboratories Japan or CLEA Japan. *Il2rg*<sup>-/-</sup>*Rag2*<sup>-/-</sup> mice (#4111) and B6.SJL mice (#4007) were obtained from Taconic Biosciences. All mice used in the studies were 8–20 wk of age, with the exception of mice used for the isolation of ILC2s. *Zfp36*<sup>-/-</sup> mice were generated using the CRISPR/Cas9 genome editing technique. Sequences and positions of single guide RNA are shown in Fig. S2 B. The single guide RNA and mRNA encoding Cas9 were coinjected into the cytoplasm of fertilized C57BL/6N eggs, which were then transferred into the oviducts of pseudopregnant Jcl:ICR female mice. Offspring were screened by DNA sequencing, and founder offspring containing a premature stop codon in exon 2 via frame-shift mutation (Fig. S2 A) were selected for establishing the mouse line. All experiments were approved by the animal care and use committee of RIKEN or Osaka University and were performed in accordance with institutional guidelines.

### Cell preparation

Cells were isolated from the spleen, mesentery, lungs, and SI of mice. The spleen was smashed through a 70- $\mu$ m nylon mesh,

and spleen cells were used for flow cytometry analysis after lysis of red blood cells. The mesentery was prepared as previously described (Moro et al., 2015). The lungs were minced with scissors and digested in HBSS with 2% BSA (Sigma-Aldrich), liberase-TM (Roche), and DNase I (Roche) with agitation at 150 revolutions per minute (rpm) on a rotary shaker at 37°C for 45 min. Digested tissues were dispersed using an automated tissue dissociator (GentleMACS; Miltenyi Biotec) running program C and then passed through a 100- $\mu$ m nylon mesh. Single-cell suspensions were further purified with 30% Percoll (GE Healthcare) after lysis of red blood cells for flow cytometry analysis and cell culture. The SI was stirred in PBS with 10% FCS (Bovogen Biologicals) and 5 mM EDTA at 350 rpm and 37°C for 20 min after removing feces and Peyer's patches. Floating cells were collected as the intraepithelial lymphocytes (IELs); the remaining tissue was washed with PBS and cut into small pieces with scissors and digested in RPMI-1640 (Sigma-Aldrich) with 10% FCS (Bovogen Biologicals), Collagenase IV (Sigma-Aldrich), and DNase I at 150 rpm on a rotary shaker at 37°C for 30 min. Digested tissue containing the lamina propria lymphocyte (LPL) fraction was dispersed using GentleMACS running program m\_intestine\_01 and then passed through a 100- $\mu$ m nylon mesh. The LPL and IEL fractions were further purified with 30% Percoll after lysis of red blood cells for flow cytometry analysis and cell culture.

### Antibodies and reagents

mAbs specific for mouse B220 (RA3-6B2), c-Kit (2B8), CD3 $\epsilon$  (145-2C11), CD5 (53-7.3), CD8 (53-6.7), CD11b (M1/70), CD11c (HL3), CD16/CD32 (2.4G2), CD19 (1D3), CD25 (PC61), CD34 (RAM34), CD45.1 (A20), CD45.2 (104), CD49b (DX5), CD127 (A7R34), GATA3 (L50-823), Gr-1 (RB6-8C5), MHC class II (M5/114.1), NK1.1 (PK136), Sca-1 (D7), Siglec-F (E50-2440), ST2 (U29-93), Thy1.2 (53-2.1), IL-4 (11B11), IL-12 (C15.6), IFN- $\gamma$  (XMG1.2), and fluorochrome-conjugated streptavidin were purchased from BD Biosciences. mAbs specific for mouse CD4 (GK1.5), Flt3 (A2F10), F4/80 (BM8), IL-5 (TRFK5), IL-17RB (9B10), and NKp46 (29A1.4) were purchased from BioLegend. mAbs specific for mouse  $\alpha$ 4 $\beta$ 7 (DATK32), Fc $\epsilon$ RI $\alpha$  (MAR-1), IL-13 (eBio13A), and killer cell lectin-like receptor G1 (KLRG1; 2F1) were purchased from eBioscience. mAbs against mouse CD16/CD32 (2.4G2), CD28 (37.51), and erythroid cell marker (TER-119) were purified from hybridoma culture supernatants in our laboratory.

Recombinant mouse IL-2, mIL-4, mIL-6, mIL-7, mIL-33, and mTGF- $\beta$ 1 were purchased from R&D Systems. p38 inhibitor (SB203580) and actinomycin D were purchased from Sigma-Aldrich.

### Flow cytometry

Cells were incubated with anti-CD16/CD32 to block nonantigen-specific binding of Igs to Fc $\gamma$  receptors. Propidium iodide or

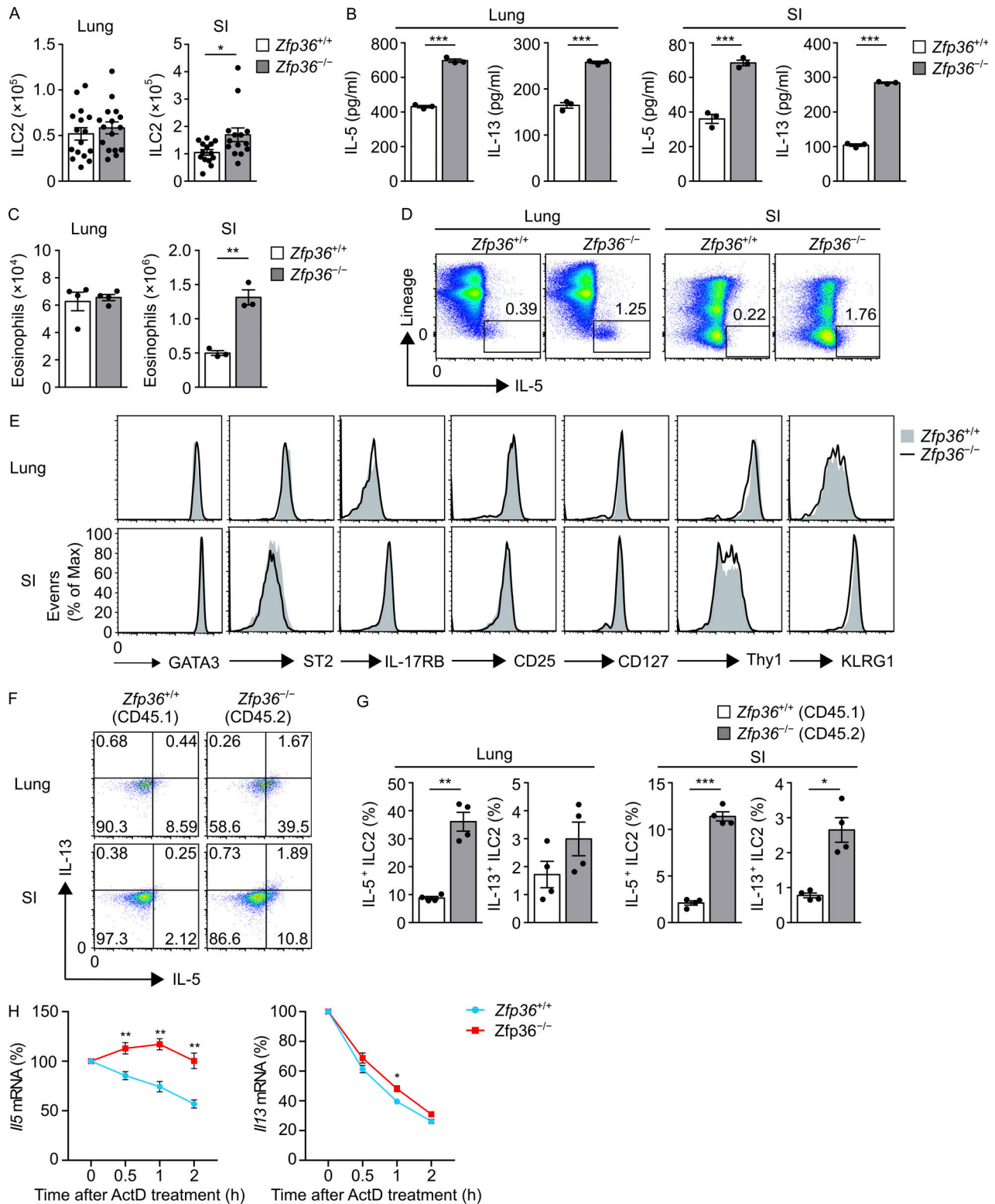


**Figure 4. TTP defect upregulates constitutive IL-5 and IL-13 production by ILC2s in vivo.** (A) Absolute number of ILC2s in the lungs and SI of *Zfp36*<sup>+/+</sup> or *Zfp36*<sup>-/-</sup> mice. (B) Concentration of IL-5 and IL-13 in the supernatants of lung ILC2s ( $1.5 \times 10^4$ ) and SI ILC2s ( $9 \times 10^3$ ) from *Zfp36*<sup>+/+</sup> and *Zfp36*<sup>-/-</sup> mice cultured with IL-7 for 48 h, as detected by ELISA. (C) Absolute number of eosinophils (CD45<sup>+</sup> Siglec-F<sup>+</sup> CD11c<sup>lo/-</sup>) from the lungs and SI of the *Zfp36*<sup>+/+</sup> or *Zfp36*<sup>-/-</sup> mice. (D) Intracellular staining of IL-5 and IL-13 in CD45<sup>+</sup> cells from the lungs and SI of the *Zfp36*<sup>+/+</sup> or *Zfp36*<sup>-/-</sup> mice. (E) Flow cytometric analysis of the expression levels of GATA3, ST2, IL-17RB, CD25, CD127, Thy1.2, and KLRG1 on ILC2s from the lungs and SI of the *Zfp36*<sup>+/+</sup> and *Zfp36*<sup>-/-</sup> mice. (F and G) BM cells from the WT (CD45.1) and *Zfp36*<sup>-/-</sup> (CD45.2) mice cotransferred (1:1) into recipient *Il2rg*<sup>-/-</sup> *Rag2*<sup>-/-</sup> mice (CD45.2). (F) Intracellular staining of IL-5 and IL-13 in *Zfp36*<sup>+/+</sup> or *Zfp36*<sup>-/-</sup> ILC2s from the lungs and SI of recipient mice at 12 wk after transfer. (G) Frequency of IL-5<sup>+</sup> and IL-13<sup>+</sup> *Zfp36*<sup>+/+</sup> or *Zfp36*<sup>-/-</sup> ILC2s from the lungs and SI of recipient mice as in F. (H) Expression levels of *Il5* and *Il13* mRNA in freshly isolated ILC2s from the lung of the *Zfp36*<sup>+/+</sup> or *Zfp36*<sup>-/-</sup> mice and treated with



actinomycin D (ActD) for 0.5, 1, and 2 h, as measured by qPCR. In A, data are pooled from four independent experiments (mean  $\pm$  SEM of  $n = 3$  or 4 mice per experiment), and in B–H, data are representative of two independent experiments (mean  $\pm$  SEM of  $n = 3$  or 4 mice). \*,  $P < 0.05$ ; \*\*,  $P < 0.01$ ; and \*\*\*,  $P < 0.001$  by Student's *t* test. Evens, event rate; Max, maximum.

Zombie Fixable Viability Dye (BioLegend) were used to detect dead cells. For intracellular cytokine staining, the cells were fixed and permeabilized using the IntraPrep Permeabilization Reagent (Beckman Coulter) according to the manufacturer's instructions. Foxp3/Transcription Factor Staining Buffer Set (eBioscience) was used for GATA3 staining. mAbs against CD3 $\epsilon$ , CD4, CD5, CD8 $\alpha$ , CD11c, CD19, Fc $\epsilon$ RI $\alpha$ , F4/80, Gr-1, NK1.1, and TER-119 were used as Lin markers for the detection of ILC2s. mAbs against CD3 $\epsilon$ , CD8 $\alpha$ , CD19, Gr-1, and TER-119 were used as Lin markers for the detection of natural killer (NK) cells, ILC1s, ILC3s, and lymphoid tissue inducer (LTi) cells. mAbs against CD3 $\epsilon$ , CD11b, CD19, F4/80, Gr-1, NK1.1, and TER-119 were used as Lin markers for the detection of GMP and common lymphoid progenitor (CLP). Lung ILC2s were gated by CD45 $^{+}$  Lin $^{-}$  GATA3 $^{+}$  or CD45 $^{+}$  Lin $^{-}$  Thy1.2 $^{+}$  ST2 $^{+}$ . SI ILC2s were gated by CD45 $^{+}$  Lin $^{-}$  GATA3 $^{+}$  or CD45 $^{+}$  Lin $^{-}$  KLRG1 $^{+}$  Sca-1 $^{-}$ . T cells were gated by CD45 $^{+}$  CD3 $^{+}$  CD19 $^{-}$  NK1.1 $^{-}$ , B cells were gated by CD45 $^{+}$  CD3 $^{-}$  CD19 $^{+}$  NK1.1 $^{-}$ , and CD11b $^{+}$  Gr-1 $^{+}$  cells were gated by CD45 $^{+}$  CD11b $^{+}$  Gr-1 $^{+}$  in the spleen and BM. GMP was gated by Lin $^{-}$  c-Kit $^{+}$  Sca-1 $^{+}$  CD34 $^{hi}$  CD16/32 $^{hi}$ , and CLP was gated by Lin $^{-}$  c-Kit $^{int}$  Sca-1 $^{int}$  CD127 $^{+}$  Flt3 $^{+}$   $\alpha$ 4 $\beta$ 7 $^{-}$  in the BM. Eosinophils were gated by SSC $^{hi}$  Siglec-F $^{hi}$  CD11c $^{lo/-}$ . ILC2s as CD45.2 $^{+}$  Lin $^{-}$  Thy1.2 $^{+}$  ST2 $^{+}$  and NK cells as CD45.2 $^{+}$  Lin $^{-}$  NK1.1 $^{+}$  were sorted from the lungs. ILC2s were sorted from the mesentery with the same markers as lung ILC2s. ILC1s as CD45 $^{+}$  Lin $^{-}$  Thy1.2 $^{+}$  NK1.1 $^{+}$  NKp46 $^{+}$  were sorted from the IEL fraction of SI. ILC2s as CD45 $^{+}$  Lin $^{-}$  KLRG1 $^{+}$  Sca-1 $^{+}$  and ILC3s as CD45 $^{+}$  Lin $^{-}$  Thy1.2 $^{+}$  KLRG1 $^{-}$  NKp46 $^{+/-}$  were sorted from the LPL fraction of SI. Macrophages as CD45 $^{+}$  CD11b $^{+}$  F4/80 $^{+}$ , CD4 $^{+}$  T cells as CD45 $^{+}$  Thy1.2 $^{+}$  CD4 $^{+}$ , NK cells as CD45 $^{+}$  Lin $^{-}$  NK1.1 $^{+}$ , and LTi cells as CD45 $^{+}$  Lin $^{-}$  Thy1.2 $^{+}$  NK1.1 $^{-}$  were sorted from the spleen. Cells were analyzed using a FACSCanto and FACSaria III (BD Biosciences) and sorted using a FACSaria IIIu. Data were analyzed using FlowJo software (TreeStar).

### In vitro ILC2 culture and cytokine quantification

For retrovirus transduction experiments, ILC2s isolated from the mesentery were first expanded in a 96-well round-bottom plate containing ILC2 culture medium (RPMI-1640 supplemented with 10% FCS [MP Biomedicals], 50  $\mu$ M 2-mercaptoethanol [Gibco], 100 U/ml penicillin and 100  $\mu$ g/ml streptomycin [Gibco], 50  $\mu$ g/ml gentamycin [Nacalai Tesque], 1 $\times$  nonessential amino acids [Sigma-Aldrich], 10 mM Hepes [Sigma-Aldrich], and 1 mM sodium pyruvate [Gibco]) with 10 ng/ml rmIL-2 and 10 ng/ml rmIL-7 at 37°C under 5% CO $_2$ . To assess cytokine production, the infected ILC2s were seeded at 5,000 cells per well into a 96-well round-bottom plate and stimulated with 10 ng/ml rmIL-2 and 10 ng/ml rmIL-33 for 72 h at 37°C under 5% CO $_2$ . The cytokine concentrations in the supernatant were measured using Bio-Plex Pro Mouse Cytokine 23-plex Assay kits (Bio-Rad).

For other cytokine production analyses, ILC2s isolated from the lungs, mesentery, and SI were seeded into 96-well round-bottom plates and stimulated in ILC2 culture medium

supplemented with 10 ng/ml rmIL-2, 10 ng/ml rmIL-7, 10 ng/ml rmIL-33, and 10  $\mu$ M SB203580 at 37°C under 5% CO $_2$ . The SI were suspended in radioimmunoprecipitation assay buffer supplemented with protease inhibitors and homogenized using a bio-masher (Nippi Collagen). The supernatants were used to determine the concentrations of IL-5 and IL-13 using Quantikine ELISA Kits or DuoSet ELISA Development Systems Kits (R&D Systems); additionally, IgA concentrations were estimated using an ELISA Quantitation Set (Bethyl Laboratories) according to the manufacturers' instructions. To assess ex vivo cytokine production, whole-lung and SI cells were incubated with Brefeldin A (Invitrogen) without stimulation for 5 h at 37°C under 5% CO $_2$ .

### Plasmid

Retroviral vector encoding *Zfp36* was cloned by inserting *Zfp36* cDNA into the pMX-IRES-GFP vector between EcoRI and XhoI sites using KOD -Plus- Neo (TOYOBO). Each 3' UTR plasmid, except *Il5* 3' UTR  $\Delta$ ARE4, was cloned by inserting each 3' UTR into the pGL3-promoter vector (Promega) in the XbaI site using KOD -Plus- Neo. *Il5* 3' UTR  $\Delta$ ARE4 was cloned using pGL3-promoter-*Il5* 3' UTR as a template using KOD -Plus- Neo. Primers for *Zfp36* cDNA (forward, 5'-CGCGAATTCATGGATCTCTCTGCC ATCTA-3'; reverse 5'-AGGCTCGAGTCACTCAGAGACAGAGAT AC-3'), *Il5* 3' UTR full (forward, 5'-AAATCTAGATGAGGCTGA GCTGCTCCATG-3'; reverse, 5'-CCGTCTAGAGAATATTATATA CGTTGTAA-3'), *Il5* 3' UTR  $\Delta$ ARE1-3 (forward, 5'-CCCTCTAGA CCTGTAGTCAGTTAAACCTATCTAT-3'; reverse, same as reverse primer of *Il5* 3' UTR full), *Il5* 3' UTR  $\Delta$ ARE4 (forward, 5'-CCCCTAGTCAATCTCTCCTCAACT-3'; reverse, 5'-AAGTTA GATAGGAGCAGGAAGCCCC-3'), *Il5* 3' UTR  $\Delta$ ARE5-7 (forward, same as primer of *Il5* 3' UTR full; reverse, 5'-GCCTCTAGACAT CTGTTTTTCTGGAGTA-3'), and *Il13* 3' UTR full (forward, 5'-CCGTCTAGATAATGAGGAGAGACCATCCC-3'; reverse, 5'-CCG TCTAGACCGGTTTCTAGTTTGACAGT-3') were used for cloning.

### Retroviral transduction

The retroviral vector pMX-IRES-GFP was transfected into PLAT-E packaging cells (a gift from T. Kitamura from the University of Tokyo, Tokyo, Japan) using FuGENE 6 (Promega) according to the manufacturer's instructions, and the culture supernatants 2 d after transfection were used as a source of viral particles. Cultured ILC2s were transduced with pMX-IRES-GFP viral particles at 1 and 2 d after stimulation with 10 ng/ml rmIL-2 and 10 ng/ml rmIL-33. After 4 d of stimulation, ILC2s were incubated with Brefeldin A for 1 h before subsection to intracellular cytokine staining. For multiplex assays, the infected cells were sorted as GFP $^{+}$  after 4 d of stimulation. For mRNA stability assays and quantification of mRNA expression, the infected cells were sorted as GFP $^{+}$  after 3 d of stimulation.

### Reverse transcription and qPCR

Total RNA was isolated with TRIzol (Thermo Fisher Scientific). cDNA was synthesized using SuperScript III Reverse Transcription

(Invitrogen) according to the manufacturer's instructions. The expression levels of *Il5* primary (forward, 5'-TCAAAATATGTG TACGTTGTGGGCA-3'; reverse, 5'-AGATTTCTCCAATGCATA GCTGGTG-3'), *Il13* primary (forward, 5'-GAGCTGAGCAACATC ACACAAG-3'; reverse, 5'-GCTTCGTCTGTCACTCACAC-3'), *Il5* (forward, 5'-AGCAATGAGACGATGAGGCT-3'; reverse, 5'-CCC ACGGACAGTTTGATTC-3'), *Il6* (forward, 5'-ACAACCACGGCC TTCCCTACTT-3'; reverse, 5'-CACGATTTCCCAGAGAACATGTG-3'), *Il13* (forward, 5'-TGTGTCTCTCCCTCTGACCC-3'; reverse, 5'-TCCAGGGCTACACAGAACC-3'), *Il33* (forward, 5'-TCCAAC TCCAAGATTTCCCG-3'; reverse, 5'-CATGCAGTAGACATGGCA GAA-3'), *Csf2* (forward, 5'-ATGCTGTACAGTTGAATGAAG-3'; reverse, 5'-GCGGGTCTGCACACATGTTA-3'), and *Zfp36* (forward, 5'-TCTGCCATCTACGAGAGCCT-3'; reverse, 5'-GTT CCAAAGTCAGGGTCCAC-3') were measured using real-time qPCR with SsoAdvanced Universal SYBR Green SuperMix (Bio-Rad) and an StepOnePlus Real-Time PCR System (Applied Biosystems). mRNA expression levels were normalized to those of *Actb* (forward, 5'-ACTATTGGCAACGAGCGGTTTC-3'; reverse, 5'-GGATGCCACAGGATTCCATAC-3').

### Stability of mRNA

ILC2s isolated from mesentery were first cultured with 10 ng/ml rmIL-33 for 2 h. Actinomycin D (5  $\mu$ g/ml) was then added to the culture medium with 10  $\mu$ M SB203580 under IL-33-stimulated condition, and total RNA was extracted at 0, 0.5, 1, and 2 h after actinomycin D treatment. In retroviral transduction analysis, the infected ILC2s were cultured with 10  $\mu$ g/ml actinomycin D, and total RNA was then extracted at 0, 1, 2, and 4 h after actinomycin D treatment. ILC2s isolated from the lung of *Zfp36*<sup>+/+</sup> and *Zfp36*<sup>-/-</sup> mice were cultured with only 10  $\mu$ g/ml actinomycin D, and total RNA was then extracted at 0, 0.5, 1, and 2 h after actinomycin D treatment. Extracted RNAs were subjected to real-time qPCR to determine *Il5*, *Il6*, and *Il13* expression levels.

### IL-33 injection

Mice were administered once i.n. with 100 ng rmIL-33 in PBS or PBS alone. At 24 and 72 h after IL-33 administration, ILC2s were sorted from the lungs of these mice for RNA extraction.

### Isolation of MEFs

Dissected mouse embryos (embryonic day [E] 15) from the uterus of plugged C57BL/6N mice were placed in a 100-mm tissue culture dish containing sterile PBS. The embryos were transferred to a clean dish with fresh PBS after removing the head and internal organs. Subsequently, embryos were transferred to a clean 100-mm tissue culture dish containing 5 ml 0.05% trypsin/EDTA solution (Gibco) and minced into small pieces using scissors. Tissues were transferred into a 50-ml tube while washing with 0.05% trypsin/EDTA up to 30 ml and incubated at 500 rpm on a rotary shaker at 37°C for 5 min. Thereafter, the contents were pipetted vigorously four times with a 25-ml pipette to lyse the digested tissues. The incubation and pipetting steps were repeated once. DMEM (Sigma-Aldrich) with 10% FCS (Bovogen Biologicals), 100 U/ml penicillin and 100  $\mu$ g/ml streptomycin, 1 $\times$  nonessential amino acids (MEF culture medium), and DNase I was added to the cell suspension.

The 50-ml tube was incubated for 15 min at 25°C to allow large tissue pieces to settle to the bottom. The supernatant was transferred, avoiding large tissue pieces, into a new 50-ml tube and centrifuged at 1,500 rpm for 5 min at 4°C. The pellet was then washed with MEF culture medium. After aspirating the supernatant, the pellet was resuspended in 10–50 ml fresh MEF medium and transferred to 100-mm tissue culture plates with approximately one embryo per plate. Media were added to a final volume of 10 ml/plate. Cells were cultured at 37°C under 5% CO<sub>2</sub> until confluent and frozen with CELLBANKER (Nippon Zenyaku Kogyo Co.). For reporter assays, MEFs that had been thawed and passaged at least once were used. MEFs were cultured in MEF complete medium at 37°C under 5% CO<sub>2</sub>.

### Reporter assay

MEFs or HEK293T cells were transfected with the pGL3-promoter plasmid combined with the pMX-IRES-GFP plasmid using FuGENE 6 according to the manufacturer's instructions and were subjected to lysis after 48 h and 24 h, respectively. Luciferase activity in the lysates was determined using the Dual-Luciferase Reporter Assay System (Promega). A *Renilla* luciferase reporter vector was also transfected and used as an internal control in every experiment. Relative luciferase activity was normalized to that of the *Renilla* luciferase.

### Western blotting

Lung tissue samples were suspended in the radioimmunoprecipitation assay buffer supplemented with protease inhibitors (Roche) and were homogenized using a biomasher (Nippi Collagens). Proteins (1 mg) were separated via SDS-PAGE and then transferred onto polyvinylidene difluoride membranes (Merck). The membranes were blocked with 5% nonfat milk in Tris buffer (pH 8.0) followed by incubation with anti-TTP (1:1,000, ABE285; Merck) and anti- $\beta$ -actin (1:1,000, sc-47778; Santa Cruz Biotechnology) in Immuno-enhancer Reagent A (Fujifilm) overnight at 4°C. After the completion of washing steps, the membranes were incubated with HRP-conjugated anti-mouse IgG (Cell Signaling Technology) and anti-rabbit IgG (Cell Signaling Technology), respectively, in Immuno-enhancer Reagent B for 1 h. After the washing steps, blots were visualized with an enhanced chemiluminescence substrate (PerkinElmer) and detected using a ChemiDoc Touch Imaging System (Bio-Rad).

### Competitive BM transplantation

Recipient *Il2rg*<sup>-/-</sup>*Rag2*<sup>-/-</sup> mice were irradiated with 2 Gy and transplanted with 5  $\times$  10<sup>6</sup> BM cells from B6.SJL (CD45.1) mice and 5  $\times$  10<sup>6</sup> BM cells from *Zfp36*<sup>-/-</sup> (CD45.2) mice. At 11–12 wk after transplantation, the indicated cells were analyzed in the lungs and SI.

### RNA sequencing

Lin<sup>-</sup> c-Kit<sup>+</sup> Sca-1<sup>+</sup> ILC2s were sorted from the mesentery of C57BL/6N mice. ILC2s were stimulated with 10 ng/ml IL-33 for 48 h to induce activation. CD4<sup>+</sup> T cells as Thy1.2<sup>+</sup> CD4<sup>+</sup>, CD8<sup>+</sup> T cells as Thy1.2<sup>+</sup> CD8<sup>+</sup>, B cells as CD19<sup>+</sup>, NK cells as NK1.1<sup>+</sup> Thy1.2<sup>-</sup>, dendritic cells as CD11b<sup>hi</sup> F4/80<sup>+</sup> Gr-1<sup>-</sup> MHC class II<sup>hi</sup> Siglec-F<sup>-</sup> CD11c<sup>hi</sup>, eosinophils as CD11b<sup>hi</sup> F4/80<sup>+</sup> Gr-1<sup>lo</sup> MHC class

II<sup>-</sup> Siglec-F<sup>+</sup> CD11c<sup>-</sup>, and macrophages as CD11b<sup>hi</sup> F4/80<sup>+</sup> Gr-1<sup>lo</sup> MHC class II<sup>-</sup> Siglec-F<sup>-</sup> CD11c<sup>-</sup> were sorted from the spleens of C57BL/6N mice. Mast cells as c-Kit<sup>+</sup> FcεRIα<sup>+</sup> CD49b<sup>-</sup> were induced from the BM cells of C57BL/6N mice by culturing with 10 ng/ml rmIL-3 for 4 wk. T cells were isolated from CD4<sup>+</sup> CD62L<sup>+</sup> splenocytes of C57BL/6N mice using the CD4<sup>+</sup> CD62L<sup>+</sup> T Cell Isolation Kit II (Miltenyi Biotec). T helper 1 (Th1) cells (cultured with 1 μg/ml anti-CD28, 10 ng/ml anti-IL-4, 10 ng/ml rmIL-12), Th2 cells (cultured with 1 μg/ml anti-CD28, 10 ng/ml anti-IL-12, 10 ng/ml anti-IFNγ, 10 ng/ml rmIL-4), and Th17 cells (cultured with 1 μg/ml anti-CD28, 30 ng/ml rmIL-6, 3 ng/ml rmTGF-β) were induced from naive T cells for 7 d on a 5 μg/ml anti-CD3ε-coated plate. LTi cells as CD19<sup>-</sup> Thy1.2<sup>+</sup> CD45<sup>+</sup> were sorted from α4β7<sup>hi</sup> c-Kit<sup>+</sup> CD127<sup>+</sup> progenitors in fetal livers (E13) cultured with 5 ng/ml rmIL-7 and TSt4/N cells for 16 d. Two independent samples were prepared for each cell population, except for dendritic cells, eosinophils, and macrophages. RNA was isolated with ISOGEN (Nippon Gene) or TRIzol LS (Thermo Fisher Scientific), and cDNA libraries were prepared using the TruSeq RNA Sample Preparation Kit v2 (Illumina) according to the manufacturer's "low sample" protocol. A HiSeq 1500 System (Illumina) was used for 50 single-end-base sequencing. Sequenced reads were trimmed for adaptor sequences and masked for low-complexity or low-quality sequences followed by mapping to the reference genome (mm9 assembly of the mouse genome) using Bowtie2 software version 2.1.0 and TopHat2 software version 2.0.8, respectively. The abundance of transcripts was estimated as fragments per kilobase of exon per million fragments mapped values using Cufflinks software version 2.1.1. EdgeR software was used to calculate differentially expressed genes and MA plots. RNA sequencing data of ILC2s, CD4 T cells, CD8 T cells, and NK cells were reported in a previous study (Miyajima et al., 2020). Data are available in the National Center for Biotechnology Information Gene Expression Omnibus under accession no. GSE184841.

### Statistical analysis

Statistical analyses were performed using GraphPad Prism 6 (GraphPad Software). Student's *t* test, with or without Welch's correction, was used to determine statistically significant differences between two groups. One-way ANOVA with the Tukey-Kramer post hoc test was used to compare more than two groups. All reported *P* values were based on two-tailed tests.

### Online supplemental material

**Fig. S1** shows the expression of *Zfp36* in ILC2s and a schematic of *Il5* and *Il13* 3' UTRs. **Fig. S2** shows additional experiments demonstrating the phenotype of *Zfp36*<sup>-/-</sup> mice.

### Acknowledgments

We thank Dr. Shigeo Koyasu from RIKEN IMS for critical reading of the manuscript and valuable suggestions; Tadashi Yamamoto and Toru Suzuki from RIKEN IMS for discussions; Satsuki Tada, Naho Hagiwara, Tomoe Shitamichi, and Yoshie Sasako for animal care; Emiko Suga, Miho Mochizuki, and Natsuki Takeno for technical support; Natsuko Otaki for

analyzing RNA sequencing data; members of the central facilities of RIKEN IMS for RNA sequencing, bio-plex analysis, and generation of *Zfp36*<sup>-/-</sup> mice; and members of the Laboratory for Innate Immune Systems at RIKEN IMS for extensive cooperation.

This study was supported by the Japan Society for Immunology Kibo Project granted to Y. Hikichi; Japan Society for the Promotion of Science (18K07187 to Y. Motomura; 16K15362 and 18H05286 to K. Moro), and Japan Agency for Medical Research and Development (16ek0410031h0001 to K. Moro).

Author contributions: Y. Hikichi designed the study, performed experiments, analyzed data, and wrote the manuscript. O. Takeuchi helped with the development of study concept. Y. Motomura and K. Moro supervised the study, planned the experiments, and wrote the manuscript.

Disclosures: The authors declare no competing interests exist.

Submitted: 22 January 2021

Revised: 5 August 2021

Accepted: 8 October 2021

### References

- Anderson, P. 2008. Post-transcriptional control of cytokine production. *Nat. Immunol.* 9:353–359. <https://doi.org/10.1038/nri1584>
- Brooks, S.A., and P.J. Blakeshear. 2013. Tristetraprolin (TTP): interactions with mRNA and proteins, and current thoughts on mechanisms of action. *Biochim. Biophys. Acta.* 1829:666–679. <https://doi.org/10.1016/j.bbarm.2013.02.003>
- Carballo, E., W.S. Lai, and P.J. Blakeshear. 1998. Feedback inhibition of macrophage tumor necrosis factor-α production by tristetraprolin. *Science.* 281:1001–1005. <https://doi.org/10.1126/science.281.5379.1001>
- Carballo, E., W.S. Lai, and P.J. Blakeshear. 2000. Evidence that tristetraprolin is a physiological regulator of granulocyte-macrophage colony-stimulating factor messenger RNA deadenylation and stability. *Blood.* 95:1891–1899. <https://doi.org/10.1182/blood.V95.6.1891>
- Chu, V.T., A. Beller, S. Rausch, J. Strandmark, M. Zänker, O. Arbach, A. Kruglov, and C. Berek. 2014. Eosinophils promote generation and maintenance of immunoglobulin-A-expressing plasma cells and contribute to gut immune homeostasis. *Immunity.* 40:582–593. <https://doi.org/10.1016/j.immuni.2014.02.014>
- Dean, J.L.E., G. Sully, A.R. Clark, and J. Saklatvala. 2004. The involvement of AU-rich element-binding proteins in p38 mitogen-activated protein kinase pathway-mediated mRNA stabilisation. *Cell. Signal.* 16:1113–1121. <https://doi.org/10.1016/j.cellsig.2004.04.006>
- Deng, K., H. Wang, T. Shan, Y. Chen, H. Zhou, Q. Zhao, and J. Xia. 2016. Tristetraprolin inhibits gastric cancer progression through suppression of IL-33. *Sci. Rep.* 6:24505. <https://doi.org/10.1038/srep24505>
- Eshelman, M.A., S.M. Matthews, E.M. Schleicher, R.M. Fleeman, Y.I. Kawasawa, D.J. Stumpo, P.J. Blakeshear, W.A. Koltun, F.T. Ishmael, and G.S. Yochum. 2019. Tristetraprolin targets *Nos2* expression in the colonic epithelium. *Sci. Rep.* 9:14413. <https://doi.org/10.1038/s41598-019-50957-9>
- Fu, M., and P.J. Blakeshear. 2017. RNA-binding proteins in immune regulation: a focus on CCCH zinc finger proteins. *Nat. Rev. Immunol.* 17:130–143. <https://doi.org/10.1038/nri.2016.129>
- Furusawa, J., K. Moro, Y. Motomura, K. Okamoto, J. Zhu, H. Takayanagi, M. Kubo, and S. Koyasu. 2013. Critical role of p38 and GATA3 in natural helper cell function. *J. Immunol.* 191:1818–1826. <https://doi.org/10.4049/jimmunol.1300379>
- Grosset, C., R. Boniface, P. Duchez, A. Solanilla, B. Cosson, and J. Ripoche. 2004. In vivo studies of translational repression mediated by the granulocyte-macrophage colony-stimulating factor AU-rich element. *J. Biol. Chem.* 279:13354–13362. <https://doi.org/10.1074/jbc.M308003200>
- Halim, T.Y.F., R.H. Krauss, A.C. Sun, and F. Takei. 2012. Lung natural helper cells are a critical source of Th2 cell-type cytokines in protease

- allergen-induced airway inflammation. *Immunity*. 36:451–463. <https://doi.org/10.1016/j.immuni.2011.12.020>
- Härde, L., M. Bachmann, F. Bollmann, A. Pautz, T. Schmid, W. Eberhardt, H. Kleinert, J. Pfeilschifter, and H. Mühl. 2015. Tristetraprolin regulation of interleukin-22 production. *Sci. Rep.* 5:15112. <https://doi.org/10.1038/srep15112>
- Jung, Y., T. Wen, M.K. Mingler, J.M. Caldwell, Y.H. Wang, D.D. Chaplin, E.H. Lee, M.H. Jang, S.Y. Woo, J.Y. Seoh, et al. 2015. IL-1 $\beta$  in eosinophil-mediated small intestinal homeostasis and IgA production. *Mucosal Immunol.* 8:930–942. <https://doi.org/10.1038/mi.2014.123>
- Kaplan, I.M., S. Morisot, D. Heiser, W.-C. Cheng, M.J. Kim, and C.I. Civin. 2011. Deletion of tristetraprolin caused spontaneous reactive granulopoiesis by a non-cell-autonomous mechanism without disturbing long-term hematopoietic stem cell quiescence. *J. Immunol.* 186:2826–2834. <https://doi.org/10.4049/jimmunol.1002806>
- Liang, J., W. Song, G. Tromp, P.E. Kolattukudy, and M. Fu. 2008. Genome-wide survey and expression profiling of CCCH-zinc finger family reveals a functional module in macrophage activation. *PLoS One.* 3:e2880. <https://doi.org/10.1371/journal.pone.0002880>
- Mesnil, C., S. Raulier, G. Paulissen, X. Xiao, M.A. Birrell, D. Pirottin, T. Janss, P. Starkl, E. Ramery, M. Henket, et al. 2016. Lung-resident eosinophils represent a distinct regulatory eosinophil subset. *J. Clin. Invest.* 126:3279–3295. <https://doi.org/10.1172/JCI85664>
- Mishra, A., S.P. Hogan, J.J. Lee, P.S. Foster, and M.E. Rothenberg. 1999. Fundamental signals that regulate eosinophil homing to the gastrointestinal tract. *J. Clin. Invest.* 103:1719–1727. <https://doi.org/10.1172/JCI6560>
- Miyajima, Y., K.N. Ealey, Y. Motomura, M. Mochizuki, N. Takeno, M. Yanagita, A.N. Economides, M. Nakayama, H. Koseki, and K. Moro. 2020. Effects of BMP7 produced by group 2 innate lymphoid cells on adipogenesis. *Int. Immunol.* 32:407–419. <https://doi.org/10.1093/intimm/dxaa013>
- Moro, K., T. Yamada, M. Tanabe, T. Takeuchi, T. Ikawa, H. Kawamoto, J. Furusawa, M. Ohtani, H. Fujii, and S. Koyasu. 2010. Innate production of T(H)2 cytokines by adipose tissue-associated c-Kit(+)-Sca-1(+) lymphoid cells. *Nature.* 463:540–544. <https://doi.org/10.1038/nature08636>
- Moro, K., K.N. Ealey, H. Kabata, and S. Koyasu. 2015. Isolation and analysis of group 2 innate lymphoid cells in mice. *Nat. Protoc.* 10:792–806. <https://doi.org/10.1038/nprot.2015.047>
- Moro, K., H. Kabata, M. Tanabe, S. Koga, N. Takeno, M. Mochizuki, K. Fukunaga, K. Asano, T. Betsuyaku, and S. Koyasu. 2016. Interferon and IL-27 antagonize the function of group 2 innate lymphoid cells and type 2 innate immune responses. *Nat. Immunol.* 17:76–86. <https://doi.org/10.1038/ni.3309>
- Neill, D.R., S.H. Wong, A. Bellosi, R.J. Flynn, M. Daly, T.K.A. Langford, C. Bucks, C.M. Kane, P.G. Fallon, R. Pannell, et al. 2010. Nuocytes represent a new innate effector leukocyte that mediates type-2 immunity. *Nature.* 464:1367–1370. <https://doi.org/10.1038/nature08900>
- Nussbaum, J.C., S.J. Van Dyken, J. von Moltke, L.E. Cheng, A. Mohapatra, A.B. Molofsky, E.E. Thornton, M.F. Krummel, A. Chawla, H.-E. Liang, and R.M. Locksley. 2013. Type 2 innate lymphoid cells control eosinophil homeostasis. *Nature.* 502:245–248. <https://doi.org/10.1038/nature12526>
- Price, A.E., H.-E. Liang, B.M. Sullivan, R.L. Reinhardt, C.J. Easley, D.J. Erle, and R.M. Locksley. 2010. Systemically dispersed innate IL-13-expressing cells in type 2 immunity. *Proc. Natl. Acad. Sci. USA.* 107:11489–11494. <https://doi.org/10.1073/pnas.1003988107>
- Qi, M.-Y., Z.-Z. Wang, Z. Zhang, Q. Shao, A. Zeng, X.-Q. Li, W.-Q. Li, C. Wang, F.-J. Tian, Q. Li, et al. 2012. AU-rich-element-dependent translation repression requires the cooperation of tristetraprolin and RCK/P54. *Mol. Cell. Biol.* 32:913–928. <https://doi.org/10.1128/MCB.05340-11>
- Qian, X., H. Ning, J. Zhang, D.F. Hoft, D.J. Stumpo, P.J. Blakeshear, and J. Liu. 2011. Posttranscriptional regulation of IL-23 expression by IFN- $\gamma$  through tristetraprolin. *J. Immunol.* 186:6454–6464. <https://doi.org/10.4049/jimmunol.1002672>
- Ricardo-Gonzalez, R.R., S.J. Van Dyken, C. Schneider, J. Lee, J.C. Nussbaum, H.-E. Liang, D. Vaka, W.L. Eckalbar, A.B. Molofsky, D.J. Erle, and R.M. Locksley. 2018. Tissue signals imprint ILC2 identity with anticipatory function. *Nat. Immunol.* 19:1093–1099. <https://doi.org/10.1038/s41590-018-0201-4>
- Sauer, I., B. Schaljo, C. Vogl, I. Gattermeier, T. Kolbe, M. Müller, P.J. Blackshear, and P. Kovarik. 2006. Interferons limit inflammatory responses by induction of tristetraprolin. *Blood.* 107:4790–4797. <https://doi.org/10.1182/blood-2005-07-3058>
- Sedlyarov, V., J. Fallmann, F. Ebner, J. Huemer, L. Sneezum, M. Ivin, K. Kreiner, A. Tanzer, C. Vogl, I. Hofacker, and P. Kovarik. 2016. Tristetraprolin binding site atlas in the macrophage transcriptome reveals a switch for inflammation resolution. *Mol. Syst. Biol.* 12:868. <https://doi.org/10.15252/msb.20156628>
- Seillet, C., K. Luong, J. Tellier, N. Jacquolot, R.D. Shen, P. Hickey, V.C. Wimmer, L. Whitehead, K. Rogers, G.K. Smyth, et al. 2020. The neuropeptide VIP confers anticipatory mucosal immunity by regulating ILC3 activity. *Nat. Immunol.* 21:168–177. <https://doi.org/10.1038/s41590-019-0567-y>
- Stoecklin, G., S.A. Tenenbaum, T. Mayo, S.V. Chittur, A.D. George, T.E. Baroni, P.J. Blakeshear, and P. Anderson. 2008. Genome-wide analysis identifies interleukin-10 mRNA as target of tristetraprolin. *J. Biol. Chem.* 283:11689–11699. <https://doi.org/10.1074/jbc.M709657200>
- Taylor, G.A., E. Carballo, D.M. Lee, W.S. Lai, M.J. Thompson, D.D. Patel, D.I. Schenkman, G.S. Gilkeson, H.E. Broxmeyer, B.F. Haynes, and P.J. Blakeshear. 1996. A pathogenetic role for TNF  $\alpha$  in the syndrome of cachexia, arthritis, and autoimmunity resulting from tristetraprolin (TTP) deficiency. *Immunity.* 4:445–454. [https://doi.org/10.1016/S1074-7613\(00\)80411-2](https://doi.org/10.1016/S1074-7613(00)80411-2)
- Venigalla, R.K.C., and M. Turner. 2012. RNA-binding proteins as a point of convergence of the PI3K and p38 MAPK pathways. *Front. Immunol.* 3:398. <https://doi.org/10.3389/fimmu.2012.00398>
- Zhao, W., M. Liu, N.J. D’Silva, and K.L. Kirkwood. 2011. Tristetraprolin regulates interleukin-6 expression through p38 MAPK-dependent affinity changes with mRNA 3’ untranslated region. *J. Interferon Cytokine Res.* 31:629–637. <https://doi.org/10.1089/jir.2010.0154>
- Zhao, X.-K., P. Che, M.-L. Cheng, Q. Zhang, M. Mu, H. Li, Y. Luo, Y.-D. Liang, X.-H. Luo, C.-Q. Gao, et al. 2016. Tristetraprolin down-regulation contributes to persistent TNF-Alpha expression induced by cigarette smoke extract through a post-transcriptional mechanism. *PLoS One.* 11:e0167451. <https://doi.org/10.1371/journal.pone.0167451>
- Zhu, P., X. Zhu, J. Wu, L. He, T. Lu, Y. Wang, B. Liu, B. Ye, L. Sun, D. Fan, et al. 2019. IL-13 secreted by ILC2s promotes the self-renewal of intestinal stem cells through circular RNA circPan3. *Nat. Immunol.* 20:183–194. <https://doi.org/10.1038/s41590-018-0297-6>

## Supplemental material

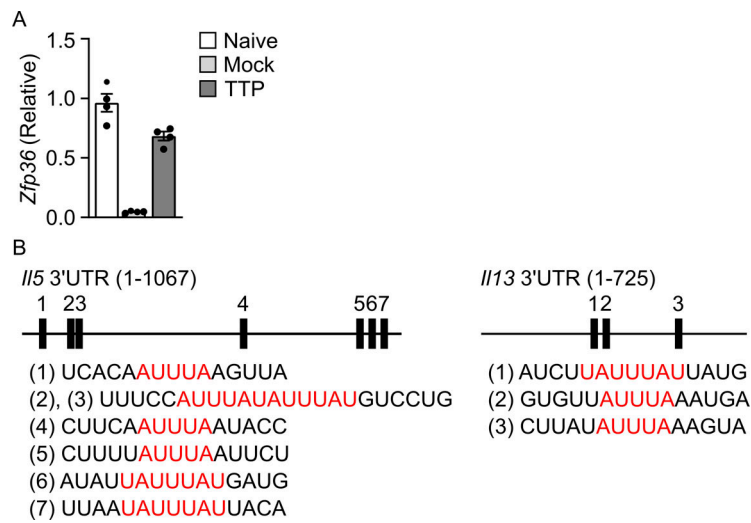


Figure S1. **TTP overexpression in ILC2s and 3' UTR of *Il5* and *Il13*.** (A) Expression levels of *Zfp36* in freshly isolated ILC2s from the mesentery and in the infected ILC2s as shown in Fig. 3 A were measured by qPCR. (B) Schematic of *Il5* and *Il13* 3' UTR. AREs indicated in red.

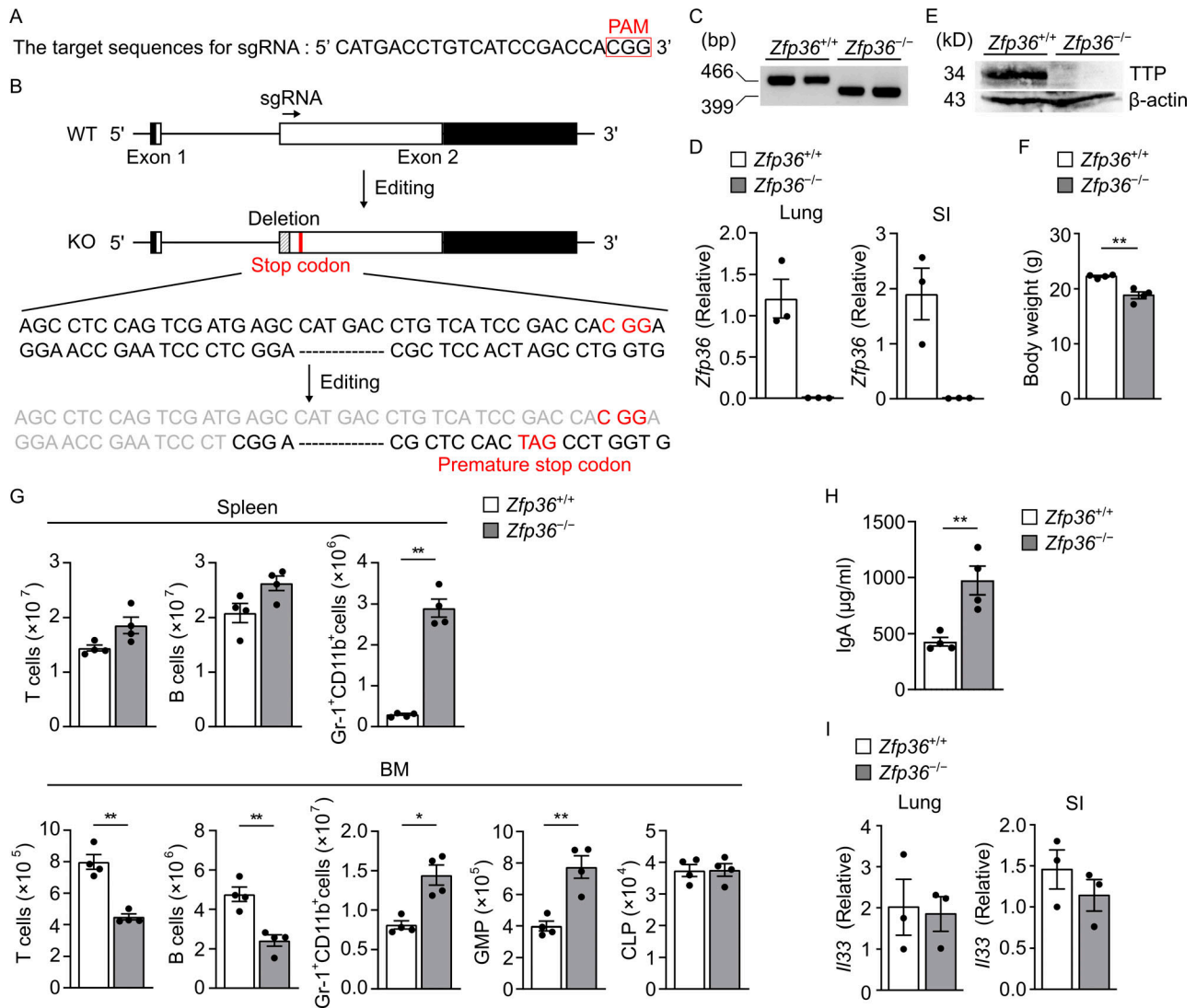


Figure S2. **Generation and phenotypic analysis of *Zfp36*<sup>-/-</sup> mice.** (A) Single guide RNA (sgRNA) target sequences. (B) Scheme of the *Zfp36* allele. The *Zfp36* cleavage sites were genetically trimmed using CRISPR/Cas9-mediated homology-directed repair. The *Zfp36*<sup>-/-</sup> allele contains a premature stop codon in exon 2. (C) Genomic PCR analysis was performed using genomic DNA derived from the tail of *Zfp36*<sup>+/+</sup> or *Zfp36*<sup>-/-</sup> mice. The *Zfp36*<sup>+/+</sup> and *Zfp36*<sup>-/-</sup> alleles were detected as 466-bp and 399-bp PCR products, respectively. (D) Expression levels of *Zfp36* in the lung tissues and SI of *Zfp36*<sup>+/+</sup> and *Zfp36*<sup>-/-</sup> mice, as measured by qPCR. (E) Western blot analysis of TTP protein levels in the SI of *Zfp36*<sup>+/+</sup> and *Zfp36*<sup>-/-</sup> mice. (F) Body weights of the 12-wk-old male *Zfp36*<sup>+/+</sup> and *Zfp36*<sup>-/-</sup> mice. (G) Absolute numbers of T cells, B cells, CD11b<sup>+</sup>Gr-1<sup>+</sup> cells, GMPs, and CLPs in the spleen and BM of the *Zfp36*<sup>+/+</sup> and *Zfp36*<sup>-/-</sup> mice. (H) Concentrations of secreted IgA in the SI of *Zfp36*<sup>+/+</sup> and *Zfp36*<sup>-/-</sup> mice, as detected by ELISA. (I) Expression of *Il33* in the whole-lung samples and SI of *Zfp36*<sup>+/+</sup> and *Zfp36*<sup>-/-</sup> mice, as measured by qPCR. Data are representative of two independent experiments (mean ± SEM of *n* = 3 or *n* = 4 in D and G-I). \*, *P* < 0.05; \*\*, *P* < 0.01.